Int J Adv Manuf Technol (2013) 67:785–795
DOI 10.1007/s00170-012-4522-4

ORIGINAL ARTICLE

Effect of waterjet peening on aluminum alloy 5005

Azmir Azhari · Christian Schindler · Bo Li

Received: 30 May 2012 / Accepted: 14 September 2012 / Published online: 26 September 2012

Abstract The present study addresses the effect of waterjet peening parameters on aluminum alloy 5005. The approach was based on the response surface methodology utilizing the Box–Behnken experimental design. Workable empirical models were developed to predict surface roughness (R_a) and hardness (HV). Increasing the number of passes, pressure, and standoff distance produces a higher surface roughness as well as a higher hardness. On the contrary, increasing the feedrate produces a lower surface roughness and hardness. The developed empirical models for R_a and HV have reasonable correlations between the measured and predicted responses with acceptable coefficients of determinations. A different set of optimum parameters was generated based on different desirability functions for each response. The predicted and the actual responses for optimized R_a and HV are satisfactory with good reliability. It is shown that the models are workable in predicting the responses of R_a and HV in the present research. A proper selection of peening parameters can be formulated to be used in practical works.

Keywords Waterjet peening · Aluminum alloy 5005 · Surface roughness · Hardness · Empirical models

1 Introduction

The technology and applications of high pressure waterjet have been studied since many decades ago. There are various applications involving waterjet technology such as machining, surface preparation, cleaning, coating removal, and surface treatment or waterjet peening (WJP). In machining processes, high-pressure waterjet is used to cut workpieces. With an addition of abrasive particles, the machining capability of waterjet is significantly improved. Different machining processes are possible including cutting, drilling, milling, etc. A whole variety of materials and thicknesses can be cut with good cutting quality and small taper. However, different processing parameters and material properties have to be carefully assessed as to produce the desired cutting qualities. Using water only at a relatively low pressure, cleaning of surfaces from dirt or coats can be achieved [1]. High pressure waterjet also is used successfully to mill coal into powders [2].

WJP is a relatively new application of the waterjet technology. It is a mechanical surface-strengthening process where high-frequent impact of water drops on the surface of metal components, which causes local plastic deformation of the metal. As a result, high compressive residual stresses are induced in the surface-near layer, which leads to an enhanced surface hardness and fatigue life of components. With an addition of abrasive particles, a higher amount of compressive residual stresses are induced together with a significant increase in roughness of metal surfaces [3]. Ramulu and Arola [4] described about various aspects of input parameters, i.e., hydraulic parameters, abrasive properties, nozzle geometry, machine parameters, and work/target material that can influence the quality of machined surfaces. Jet velocity (and flow rate), nozzle geometry, and inclination angle of attack are the main parameters influencing the jet coherence as well as cutting power whereas, stand-off distance and traverse speed of the nozzle are the main parameters affecting the interaction between the jet and workpiece surfaces [5].

Waterjet peening has shown to be a promising method in mechanical surface-strengthening process. However, a detailed knowledge of this process is not comprehensively reported in the literature. Other peening processes are widely

A. Azhari (✉) · C. Schindler · B. Li
Chair of Design in Mechanical Engineering,
University of Kaiserslautern,
67663 Kaiserslautern, Germany
e-mail: azmir.azhari@gmail.com

C. Schindler
e-mail: schindler@mv.uni-kl.de

B. Li
e-mail: whoop_boom@hotmail.com

established such as shot peening and laser shock peening. Shot peening has been extensively used in the industry. The process involves inducement of residual stresses through bombardment of the part surface with spherical shots made of hardened cast steel, glass, or ceramic beads at a relatively high velocity [6]. However, there are possible disadvantages of the process including defects and rough peened surfaces which have shown to be detrimental to fatigue crack initiation [7]. In contrast, laser shock peening involves the generation of high-pressure shock pulses by a high intensity laser in a nanosecond-pulse duration at material's surface [8]. The high intensity laser with short pulses may alter material properties by inducing tamped plasmas at the point of laser impingement. Such plasmas produce high amplitude shock waves generated at the surface that propagate into the interior of the target which subsequently induces residual stresses [8]. However, there are possibilities of thermal effects such as melting of the metal surface, especially for alloys of a low melting point [9].

Water jet peening may overcome the limitations of other peening processes, particularly leaving a clean and smooth surface with low surface roughness as well as the absence of thermal effects [10]. If the waterjet nozzle is attached to a robotic manipulator, then it is possible to treat components with complex geometries. Therefore, over the past decade, a lot of research has been conducted to study its potential applications and associated sciences. Chillman et al. [11] explored the effects of high-pressure WJP at 600 MPa on the surface finish and integrity of titanium alloy (Ti-6Al-4 V). They found that WJP at 600 MPa induces a plastic deformation to greater depths in the subsurface layer and also a higher degree of plastic deformation. Grinspan and Gnanamoorthy [10] substituted water with oil in a peening process of aluminum alloy where the depth of residual stress was noticed to be more than 250 μm below the surface. Ju and Han [12] investigated the influence of water cavitation peening (WCP) treatment on the microstructure of pure titanium. WCP refers to a technique in waterjet peening process in which suitable air can be aerated into the extra high-velocity flow in the nozzle, thereby forming a tremendous pressure gradient between the upstream and downstream flows consequently imparting a higher, deeper stress onto the surface [12]. It was observed that longer exposure time of WCP produces higher residual stresses. Qin et al. [13] investigated the influence of incidence angles on the process capability of water cavitation peening. They found that the impact pressure and residual stresses obtained at various incidence angles were almost equal to each other within the effective process area.

Considerable work has been done in investigating the effect of various WJP parameters on the inducement of residual stresses on metallic surfaces. However, little attention has been paid to the optimization of the waterjet peening process. It is known that increasing the energy and frequency of water drops may lead to a higher increase in hardness as well as a deeper hardening layer [14]. Unfortunately, it may also increase the roughness of material surfaces which is detrimental to its fatigue life. Therefore, it is important to find a balance between the increase in hardness and also roughness of the material surfaces. In order to have good increase in hardness within acceptable roughness of the peened surfaces, it is necessary to employ optimization techniques to find the optimal waterjet peening conditions. Also, workable models between the hardness as well as the roughness and the peening parameters can be developed in order to plan the process in advance with high rates of reproducibility. For this reason, the response surface methodology (RSM) can conveniently be employed. The main objective of this paper is to present the investigation on the effect of WJP parameters on aluminum alloy 5005 and also to develop workable empirical models for surface roughness (R_a) and hardness (HV).

2 Experimental work

2.1 Materials and machine

Aluminum alloys are well known to possess a high strength to weight ratio. This advantage makes them suitable to be used in many industrial applications. In the present study, aluminum alloy 5005 was used largely because it was readily available in the market. Its chemical composition and mechanical properties are given in Tables 1 and 2, respectively [15].

The test plates used for the experiments have the dimension of 40×150 mm in surface area and 3 mm of thickness. The surfaces of the received specimens were already polished and film coated with an average surface roughness, R_a of 0.5 μm. Therefore, no necessary smoothing of the surfaces was needed prior to the experiments.

Each specimen was carefully clamped on the machine table. It was treated along the small dimension of the surfaces with pre-determined parameters based on the experimental design. The UHDE waterjet machine is capable of generating pressure up to 6,000 bars. It has a nozzle made of stainless steel, brass seal, and sapphire stone produced by Quick-Ohm Küpper & Co GmbH. The nozzle has a diameter of 0.3 mm. The incidence angle was set at 90° (i.e., the nozzle was perpendicular to the specimen surface). It produces a width of treated surface of approximately 0.8 mm.

Table 1 Chemical composition (weight in percent) of aluminum alloy 5005

Mg	Si	Fe	Cu	Mn	Cr	Zn	Al
0.70–1.10	0.30	0.45	0.05	0.15	0.10	0.20	Balance

Table 2 Mechanical properties of aluminum alloy 5005

Yield strength (MPa)	Tensile strength (MPa)	Elongation (%)
40	100–150	20

The process was done without the use of abrasives where surfaces free of embedded abrasive particles could be expected. The nozzle moved in a reversible direction repeatedly. There was a gap of 2 mm between each experimental run. The gap eliminates any interference that may occur between the exposed tracks of the jets.

The roughness was measured at the surface. However, microstructural analysis was done at the surface and subsurface regions. Roughness was measured using a computer-based Hommel T8000 profilometer equipped with a ball-shaped ruby stylus tip having a diameter of 5 μm and tip angle of 90°. It was obtained along the transverse direction of the treated surface with a cut-off length of 0.8 mm. The standard surface roughness parameter or arithmetic average of the absolute values (R_a) was recorded at least three times so that averages could be calculated as to minimize the variability of surface finish data. Furthermore, a non-contact optical 3D measurement system, Nanofocus μSurf explorer was used for the measurement and analysis of surfaces. The 3D structures of the surfaces were acquired using a 10× objective lens which covers a measuring field of about 1,600×1,600 μm.

A microstructural analysis was conducted using an Olympus® BX-series light microscope on polished cross-sections of specimens prior to the measurement of hardness. This is to avoid the effect of plastic deformation from the hardness indentation. The images were captured using Buehler® OmniMet image acquisition and analysis software. Subsurface hardness was measured using a computer-controlled Buehler® OmniMet MHT hardness tester. The Vickers HV was obtained as a function of depth with 10 gf load over a 15-s indentation period. An average of at least four hardness data was recorded at every depth. Hardness measurement was acquired on the cross-section of the specimen at different depths starting from roughly 25 μm beneath the eroded surface as shown in Fig. 1. The measurements were continued at different depths until a far distance of 1,000 μm.

2.2 Waterjet peening parameters

In WJP, there are a vast number of parameters affecting the quality of the results. Therefore, only a few parameters were selected to ensure the feasibility of the multipass treatment and its influence can be properly assessed. The machining parameters and their respective ranges were carefully selected based on preliminary trial runs as well as literature reviews [3, 10–14]. The effect of WJP treatment was clearly

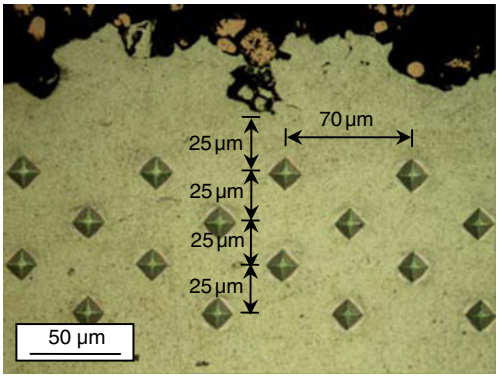

Fig. 1 Hardness measurement on a cross-sectioned specimen

observed within these ranges of parameters. The machining parameters and their ranges are shown in Table 3.

2.3 Experimental design

There are very few studies on waterjet peening that have explored on finding the optimal conditions for various peening parameters affecting the quality characteristics. Macodiyo and Soyama [16] investigated the effects of fatigue strength of carburized chrome-molybdenum steel subjected to surface treatment by cavitation peening. They used design of experiment (DOE) and RSM to model optimal conditions for the critical factors such as processing times and cavitation number affecting fatigue strength. They found that the cavitation number yielded better results in improving the fatigue strength of chrome-molybdenum steel and the models used in the DOE were in agreement with the experiments performed. Furthermore, Rajesh and Babu [17] established empirical models of waterjet peening of aluminum alloy based on Taguchi's experimental design. They noticed only a slight deviation in the results predicted with the models compared to the results obtained from the experiments.

In the present work, RSM was selected as the method for the experimental design. It is an empirical modeling approach for determining the relationship between various processing parameters and responses [18]. The Box–Behnken design is a widely used experimental design for RSM due to its simplicity [19]. It requires only parameters at three different levels and it is based on the combination of the factorial with incomplete

Table 3 Waterjet peening parameters and their respective ranges

No.	Waterjet peening parameters	Range		
		Low	Medium	High
1.	Number of passes, n	1	2	3
2.	Pressure, p (MPa)	50	100	150
3.	Feedrate, u (mm/min)	500	1,000	1,500
4.	Standoff distance, h (mm)	20	40	60

block designs for each independent parameter. Therefore, this design gives desirable statistical properties and most importantly with only a fraction of the experiments required for three-level factorials [19].

A statistical method known as multiple regression is widely used in building the empirical models in RSM. An equation is established to relate the independent parameters and the response variables [20]. A second-order empirical model is usually used in RSM as shown in Eq. 1 between the response y and independent parameters x [20],

$$y(x) = \beta_0 + \sum_{i=1}^{k} \beta_i x_i + \sum_{i=1}^{k} \beta_{ii} x_i^2 + \sum_{i} \sum_{j} \beta_{ij} x_i x_j + \varepsilon \quad (1)$$

where β and ε are the coefficients and error, respectively.

Table 4 Experimental runs and their results based on Box–Behnken experimental design

Exp. no.	Waterjet peening parameters				Responses	
	n	p (MPa)	u (mm/min)	h (mm)	R_a (μm)	Hardness ($HV_{0.01}$)
1	2	100	1,000	40	8.25	59.20
2	2	150	500	40	15.93	61.30
3	1	150	1,000	40	14.28	58.67
4	2	100	500	60	16.41	59.00
5	2	100	1,500	20	0.54	57.57
6	3	100	1,000	60	14.04	60.70
7	3	100	1,000	20	0.55	60.00
8	3	100	1,500	40	5.14	55.83
9	1	50	1,000	40	0.54	54.60
10	2	100	1,000	40	8.18	57.77
11	3	50	1,000	40	0.69	56.10
12	2	100	500	20	0.73	56.70
13	2	50	1,000	60	0.57	55.00
14	2	100	1,000	40	5.85	58.20
15	2	100	1,000	40	5.83	58.90
16	2	150	1,500	40	13.01	59.07
17	1	100	1,500	40	0.56	54.80
18	2	50	1,000	20	0.51	55.10
19	2	100	1,000	40	6.50	58.50
20	2	50	500	40	0.54	55.07
21	3	100	500	40	13.44	59.73
22	1	100	500	40	6.78	57.90
23	2	100	1,500	60	4.11	57.23
24	1	100	1,000	60	1.85	57.00
25	2	150	1,000	20	10.55	58.27
26	1	100	1,000	20	0.53	56.80
27	3	150	1,000	40	15.25	59.60
28	2	150	1,000	60	16.00	59.83
29	2	50	1,500	40	0.56	54.50

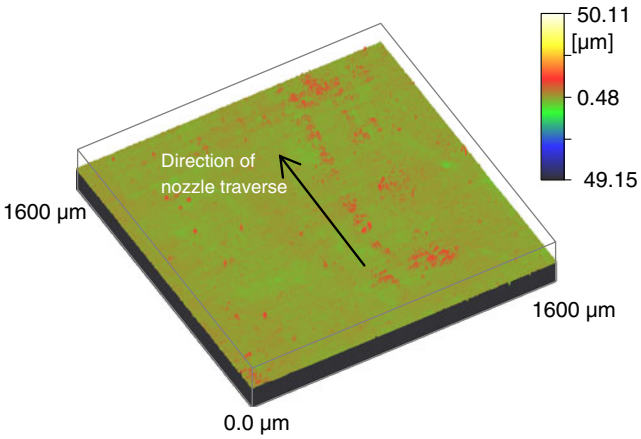

Fig. 2 3D images of surface structures for experimental run number 5 (R_a=0.54 μm)

Based on the Box–Behnken experimental design, a total of 29 experimental runs were carried out in the present study as shown in Table 4. A center point (i.e., in which all factors are at their central values) was included in the experimental design. The experimental runs for the center point were repeated five times (i.e., at experimental runs number 1, 10, 14, 15, and 19). A software for design of experiments, Design-Expert®, was used for analyzing the experimental results based on the response surface methodology approach.

3 Results and discussions

3.1 Effect of peening parameters on surface roughness

Table 4 shows the experimental results for both roughness and hardness based on the Box–Behnken experimental design. It is to note that the average original surface roughness is about 0.49 μm. In the present study, the roughnesses after the peening treatment were obtained between 0.51 and

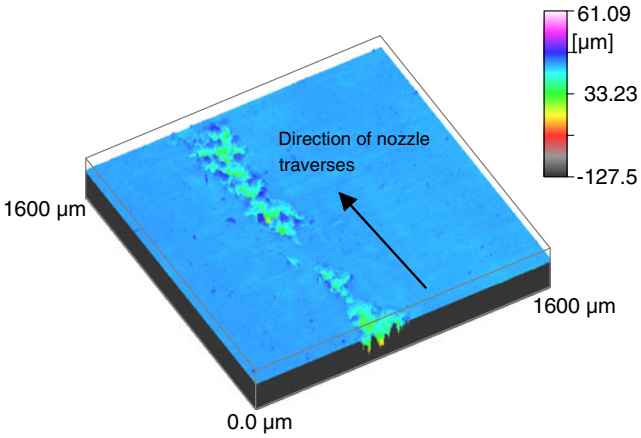

Fig. 3 3D images of surface structures for experimental run number 22 (R_a=6.78 μm)

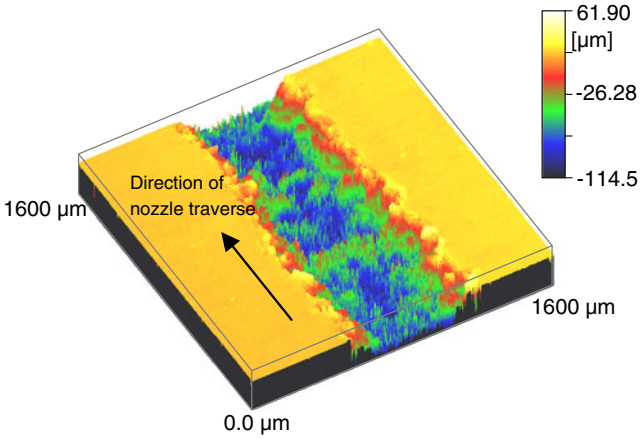

Fig. 4 3D images of surface structures for experimental run number 16 (R_a=13.78 µm)

16.42 µm. Based on the roughness level of all experimental runs, the results can be divided into three different groups. The first group consists of experimental runs with a low roughness below 1 µm. The experimental runs in the second group have a range of roughness between 1 and 10 µm. Finally, the third group refers to the experimental runs which have a high roughness of more than 10 µm.

About 11 experimental runs produce roughnesses below 1 µm. An example of a 3D image of the surface structure in this group is shown in Fig. 2. The erosions on the surfaces are hardly to be observed and they are comparable to the original surface. The amount of removed material is nearly zero. A further analysis for experimental run number 5 shows that the maximum depth of the pit was 2.90 µm. In comparison, the original surface has the maximum depth of the pit about 2.79 µm. Nevertheless, the maximum depth of the pit within this group varies from 2.80 to 4.50 µm.

About nine experimental runs have roughnesses between 1 and 10 µm. An example of 3D image of surface structure in this group is shown in Fig. 3 for the experimental run number 22. In this group, there are significant erosions over the surfaces. However, the erosion tracks are not continuous as shown in Fig. 3. Furthermore, no constant width of erosion track is produced on the surface. There is a moderate removal of material with high values of the valley-to-peak between 34.50 and 73.67 µm.

There are another nine experimental runs that produce roughnesses above 10 µm. Figure 4 shows the example of the 3D image of the surface structure for the experimental run number 16. All experimental runs in this group show severe erosions to the surfaces. There is a high amount of removed material with an almost constant width of erosion track. The erosions continue along the track without interruption with very high values of valley-to-peak in a range between 69.92 and 105.66 µm.

Figure 5 shows the effect of four different peening parameters on the surface roughnesses of the peened specimens. Overall, it can be clearly seen that increasing the number of passes produces a higher surface roughness as shown in Fig. 5a. Unlike a through cutting in a waterjet machining process, a smoothening action is expected on the side walls by subsequent passes to remove peaks left by precedent passes [21]. However, in the waterjet peening process, rougher surfaces are expected due to repeated bombardment of waterjet onto the surface [14]. This implies the roughening action on the surface by the subsequent passes which make the surface rougher.

It can be clearly seen that the surface roughness also increases with an increase in pressure as illustrated in Fig. 5b. It is known that the water supply pressure is directly proportional to the impingement velocity of the water droplet. Therefore, it can be anticipated that a higher water supply pressure increases the kinetic energy of the water molecules and enhances their capability for material removal thus increases the surface roughness. Furthermore, rougher surfaces were also produced at lower feedrates as illustrated in Fig. 5c. This effect can be explained as decreasing the traverse rate allows additional overlap machining action and more water molecules to impinge on the surface, hence, increasing the roughness of the surface.

In addition, the surface roughness increases with an increase in standoff distance as shown in Fig. 5d. A lower standoff distance may cause very little removal of material. Probably water droplets were not generated but rather a water column or a continuous beam of waterjet [22]. The continuous water column only presses the surface of the specimen without imposing the cyclic stresses. Therefore, the impact frequency of the water column is too low to cause high erosion damage at the short standoff distance [22].

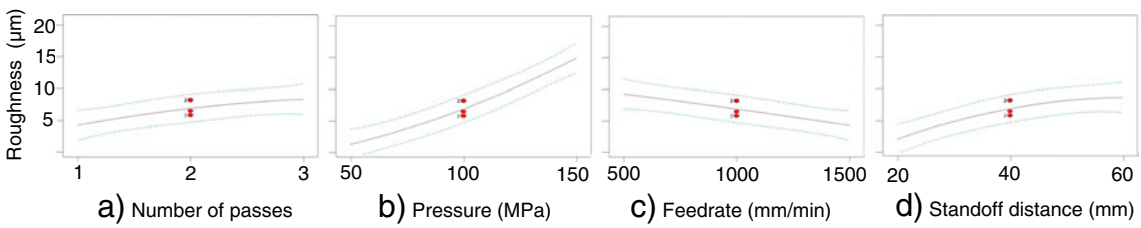

Fig. 5 Effect of **a** number of passes, **b** pressure, **c** feedrate, and **d** standoff distance on R_a

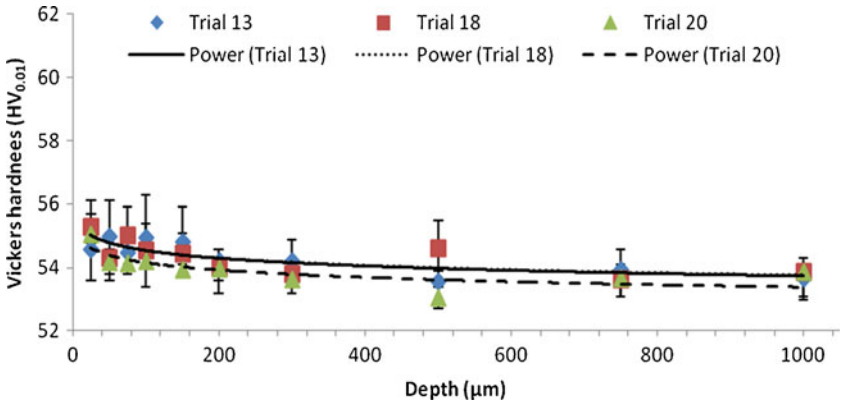

Fig. 6 Hardness as a function of depth for experimental runs with low R_a

Moreover, there is a high possibility that at a shorter standoff distance, the reflection of water droplets disturbs the new incoming water droplets from the nozzle. However, at a higher standoff distance due to the divergence of waterjet, the effect of waterjet reflection has been reduced. This explains higher erosion at higher standoff distance in the present study. It is also good to note that the maximum erosion is to be attained up to a certain distance before the erosion rate decreases again with further increase in standoff distance. Oka et al. [22] and Chillman et al. [23] found the distances to be approximately between 100 and 200 mm in waterjet treatment of aluminum alloy 5083 and titanium alloy Ti6Al4V, respectively. It is simply because a very high increase in the standoff distance results in an increase of jet diameter and in turn reduces the kinetic energy density of the jet at impingement [24].

3.2 Effect of peening parameters on hardness

On the basis of the three different groups discussed above, the effect of surface roughness on hardness was analyzed. It is to note that the base material has an average hardness of approximately 53.58 $HV_{0.01}$. Figure 6 shows the change in hardness as a function of the depth below the eroded surface for a few experimental runs which produced roughnesses below 1 µm. The roughnesses for trial 13, 18, and 20 are 0.57, 051, and 054 µm, respectively. Overall, there are almost no changes in hardness values along the depth. It may seem to be a very small change of hardness gradients near to the surface. But, the error bars are quite long to strongly suggest that there is any change in hardness gradients in the present study.

The changes of hardness gradients for experimental runs which have intermediate roughnesses (between 1 and 10 µm) are shown in Fig. 7. The roughnesses for trial 8, 22, and 23 are 5.14, 6.78, and 4.11 µm, respectively. The magnitude of hardness is high at the surface and decreases with increasing depth from the surface. There are significant changes in hardness values up to a depth of approximately 200 µm. Beyond this depth, the hardness is about the same as the original hardness at the surface.

The changes of hardness gradients for the experimental runs which produced high roughnesses (above 10 µm) are shown in Fig. 8. The roughnesses for trial 16, 27, and 28 are 13.01, 15.25, and 16.00 µm, respectively. There are significant changes in hardness values up to a depth of approximately 300 µm. It is more interesting to note that the maximum increase in hardness is not located just below the eroded surface. The maximum increase in hardnesses was recorded at a depth of approximately 80–120 µm. Further analysis of the material structures below the eroded surfaces show some cracks as can be seen in Fig. 9. The low strength of aluminum alloy makes it possible for the occurrence of cracks especially at very high impact energy

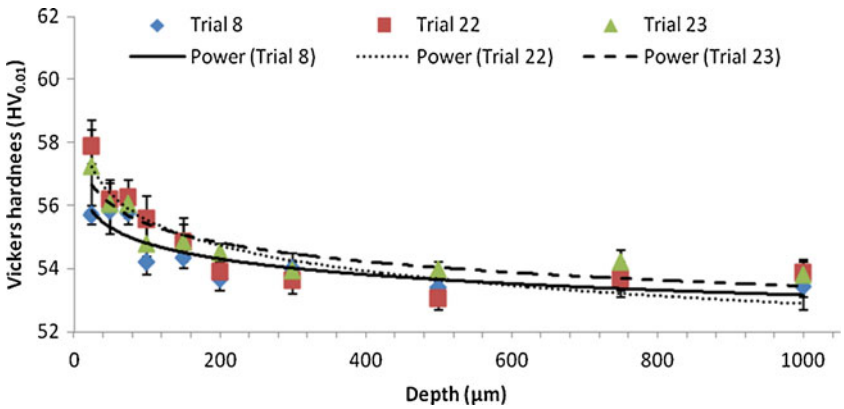

Fig. 7 Hardness as a function of depth for experimental runs with intermediate R_a

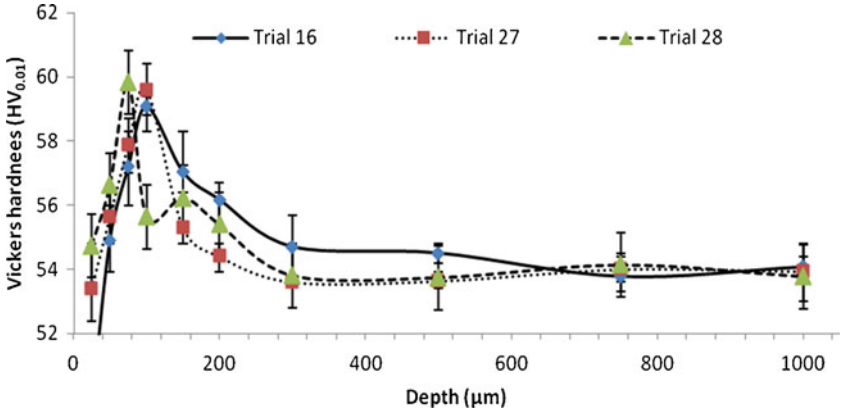

Fig. 8 Hardness as a function of depth for experimental runs with high R_a

of injected water used within this experiment. The crack propagation extends up to a depth of about 50–80 μm. Therefore, the measurement of hardness within these depths shows a low value as shown in Fig. 8.

The effect of different peening parameters on hardness is shown in Fig. 10. Overall, there is a change in maximum hardness with an increasing number of passes as shown in Fig. 10a. The increase in hardness is the result of the introduction of compressive stresses from repeated waterjet impact forces at a higher number of passes [14]. The effect of pressure on the Vickers hardness is shown in Fig. 10b. A higher hardness gradient is found in a specimen treated with a higher pressure. This is due to the fact that a higher kinetic energy of water droplets at higher pressures induces a higher amount of compressive stresses hence, increasing the hardness. Figure 10c shows the effect of the feedrate on the hardness. Increasing the traverse rate allows less water droplets to impinge on the surface. Therefore, it may induce a lower amount of compressive residual stresses and lead to a lower hardness. Besides, Figure 10d shows the effect of the standoff distance on the hardness. There is a mild increase in hardness as the standoff distance increases. It is due to the same reason above that the impact energy of waterjet is low at a lower distance because of water column effect.

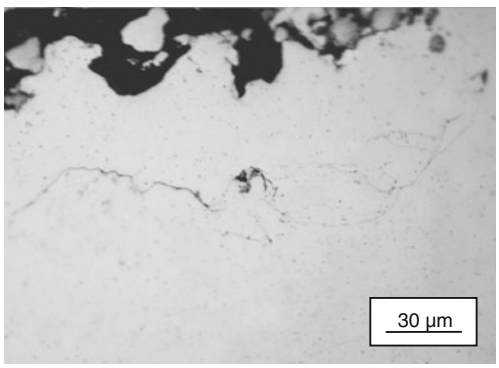

Fig. 9 Cracks below the eroded surface (Experimental run 27)

3.3 Development of empirical equations

Based on the experimental data set in Table 4, the R_a and HV empirical models were developed. The R_a model describes the average roughness on the surface while the HV model shows the maximum of the hardness value below the surface. The hardness for every trial run was measured across the specimen depth. An average of at least four hardness data was recorded at every depth. Therefore, for the purpose of developing a model for hardness, only a single value of hardness is needed for every trial run. So only the maximum hardness (average) value at a certain depth for each trial run was recorded in Table 4. Thus, the empirical model for hardness is capable to predict only the maximum hardness after the peening process regardless of the depth of hardening layer. The coefficients of regression were determined using the stepwise method of the Design Expert software. The two models were based on the 29 experimental runs conducted according to the Box–Behnken experimental design. The second-order models for R_a and HV in terms of waterjet peening parameters are shown in Eqs. 2 and 3, respectively.

$$R_a = -12.774 - 4.038n + 1.360 \times 10^{-1}p + 7.130 \times 10^{-3}u + 1.634 \times 10^{-1}h + 1.521 \times 10^{-1}nh - 3.0 \times 10^{-4}uh \quad (2)$$

$$HV = 47.908 + 1.016n + 1.092 \times 10^{-1}p + 3.15 \times 10^{-3}u - 3.3 \times 10^{-4}p^2 - 2.5 \times 10^{-6}u^2 \quad (3)$$

where n, p, u, and h are the number of passes, pressure (megapascal), feedrate (millimeters per minute), and standoff distance (millimeters), respectively.

In order to accept the models for practical use, it is important to do some assessment to check their validity. The model validation is directed toward determining whether the model will function successfully in its intended

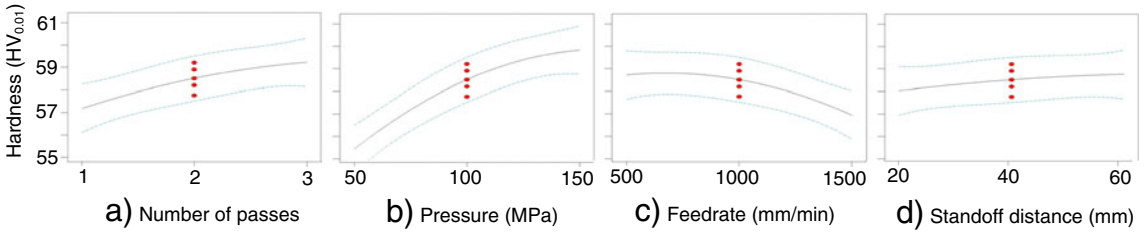

Fig. 10 Effect of **a** number of passes, **b** pressure, **c** feedrate, and **d** standoff distance on hardness

operating environment for prediction purposes. A common way for checking the validity of a regression model is by evaluating the coefficients of determinations (R^2 and adjusted R^2) [20]. It is the proportion of variation explained by the regressor where values of that are close to 1 mean that most of the variability in response is explained by the regression model. Generally, if the model fits the data well, the overall value of R^2 and adjusted R^2 $\left(R^2_{adj}\right)$ should be greater or equal to 0.70. For the case of surface roughness, the values of R^2 and R^2_{adj} are 0.884 and 0.852, respectively. Whereas, the values of R^2 and R^2_{adj} for hardness are 0.808 and 0.766, respectively. It is believed that both models have reasonable correlations between the measured and the predicted values for R_a and HV. Therefore, the empirical models are useful in predicting the responses of R_a and HV during waterjet peening of aluminum alloy 5005 within the ranges of the parameters in this study. A proper selection of the peening parameters can be formulated to be used in practical works.

The significance of the models and their parameters were then investigated through the analysis of variance (ANOVA). ANOVA is a statistical technique conducted mainly to learn about the influence of various design parameters and to observe the degree of sensitivity of the result to different parameters affecting the quality characteristics [25]. A larger F value indicates that there is a big change in the performance characteristic due to the variation of the process parameter. Also, if a p value of any model and its terms is less than or equal to 0.05, the terms in the model have significant effect on the response. Tables 5 and 6 show the ANOVA results for R_a and HV, respectively. This analysis was carried out for a 95 % confidence level. It was found that the respective p values for both models are less than 0.05. It shows that both models are significant.

Based on the p value for the R_a model as shown in Table 5, all the model terms are significant with pressure having the highest degree of significance followed by standoff distance, feedrate, and number of passes. Furthermore, the interactions either between the number of passes and the standoff distance as well as between the feedrate and the standoff distance are also significant but they have a low degree of significance on the surface roughness. It is also good to note that as discussed above, none of the experimental runs with roughnesses below 10 μm were treated with the highest pressure of 150 MPa. This simply confirms that the pressure is the most significant parameter in influencing the surface roughness in this experiment. Hence, treating the surfaces with the highest pressure will certainly produce extensively rougher surfaces.

The p value of the lack of fit test is 0.08. It is insignificant since its value is more than 0.05 thus indicating that all the data in this study fit the model adequately. The individual

Table 5 ANOVA results for surface roughness (R_a)

Source	Sum of squares	Degree of freedom	Mean square	F value	p value ($prob > F$)
Model	884.046	6	147.341	27.826	<0.0001
n	50.307	1	50.307	9.501	0.0054
p	555.016	1	555.016	104.816	<0.0001
u	74.551	1	74.507	14.079	0.0011
h	130.482	1	130.482	24.641	<0.0001
nh	37.027	1	37.027	6.992	0.0148
uh	36.663	1	36.663	6.923	0.0152
Residual	116.493	22	5.295	–	–
Lack of fit	110.627	18	6.146	4.191	0.0872
Pure error	5.866	4	1.466	–	–
Cor total	1,000.539[a]	28[b]	–	–	–

Prob probability, *Cor total* corrected total

[a]Corrected total = total sum of squares (SS) for the model terms + Residual SS

[b]Corrected total = sum of degrees of freedom (*df*) of all the model terms + residual *df*

Table 6 ANOVA results for hardness (HV)

Source	Sum of squares	Degree of freedom	Mean square	*F* value	*p* value (prob>*F*)
Model	86.254	5	17.251	19.319	<0.0001
n	12.383	1	12.383	13.867	0.0011
p	57.948	1	57.948	64.894	<0.0001
u	9.541	1	9.541	10.684	0.0034
P^2	4.590	1	4.590	5.140	0.0331
u^2	2.625	1	2.625	2.940	0.0999
Residual	20.538	23	0.893	–	–
Lack of Fit	19.266	19	1.014	3.189	0.1347
Pure error	1.272	4	0.318	–	–
Cor total	106.793	28	–	–	–

Prob probability, *Cor total* corrected total

[a]Corrected total = total sum of squares (SS) for the model terms + Residual SS

[b]Corrected total = sum of degrees of freedom (*df*) of all the model terms + residual *df*

influence of each parameter on R_a was discussed above. However, it is interesting to discuss about the significant interaction effects between the number of passes and the standoff distance as well as between the feedrate and the standoff distance. As shown in Table 5, both interactions are significant as indicated by the *p* values which are less than 0.05. The effect of interaction between the number of passes and the standoff distance on R_a is shown in Fig. 11. It can be observed that at a lower number of passes, R_a shows only marginal changes at different levels of the standoff distance. However, at the highest number of passes, R_a increases dramatically as the standoff distance increases from 20 to 60 mm. This indicates that in this study there exists a strong interaction between the number of passes and the standoff distance particularly at a higher level of jet passes. On the contrary, the interaction between the feedrate and the standoff distance shows a reverse effect on surface roughness as shown in Fig. 12. In other words, the effect of increasing the standoff distance on R_a is more profound at the lowest feedrate. R_a increases significantly while the standoff distance increases from 20 to 60 mm at the lowest feedrate. However, changing the standoff distance shows an almost no change in R_a at the highest feedrate of 1,500 mm/min. Similarly, R_a does not change with increasing feedrate at the lowest standoff distance of 20 mm. This suggests that there is a strong interaction between the feedrate and the standoff distance in influencing the R_a.

Whereas, based on the *p* value for the HV model as shown in Table 6, all the parameters are significant except the standoff distance. Again, the pressure has the highest degree of significance followed by the number of passes and the feedrate. As presented in Table 4 above, the highest HV recorded was at the highest pressure of 150 MPa. Also, the values of HV were notably higher at the highest pressure. This simply confirms that the pressure is the most significant parameter in influencing the HV in this experiment.

The *p* value of the lack of fit test is 0.13. It is insignificant since its value is more than 0.05 thus indicating that all the data fit the model adequately in this study. The individual influence of each parameter on HV has been explained above. However, it is interesting to discuss the insignificant effect of the standoff distance in influencing the HV. There is a possibility that the chosen range of standoff distance (i.e., 20–60 mm) in this study gives a marginal effect to the

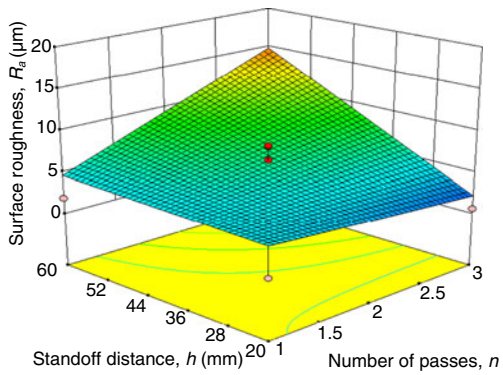

Fig. 11 Effect of interaction between number of passes and standoff distance on R_a

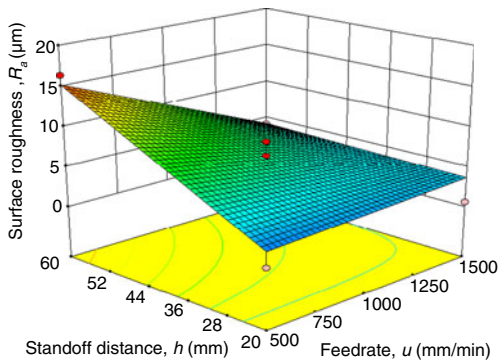

Fig. 12 Effect of interaction between feedrate and standoff distance on R_a

Table 7 Optimization runs and their results

Exp. no.	Waterjet peening parameters				Actual responses		Predicted responses	
	n	p (MPa)	u (mm/min)	h (mm)	R_a (μm)	Hardness ($HV_{0.01}$)	R_a (μm)	Hardness ($HV_{0.01}$)
1	3	130.0	735.14	24.7	8.90	59.50	7.91	60.54
2	3	122.1	784.58	20.0	4.53	58.33	5.00	60.30
3	3	114.0	806.18	20.0	2.30	58.67	3.93	60.03
4	3	108.1	818.67	20.0	1.39	58.23	3.14	59.81
5	3	103.0	826.61	20.0	0.77	57.67	2.45	59.60

HV. As found by Oka et al. [22] in waterjet treatment of aluminum alloy 5083, the value for the impingement force was constant at a standoff distance of less than 100 mm. Therefore, it gave an almost constant hardening effect to the surface of the material. Furthermore, Grinspan and Gnanamoorthy [26] found only a slight increase in HV for oil jet peened aluminum alloy 6063-T6 at different standoff distances between 25 and 40 mm. There was less than 4 % difference of the hardness increase from the original hardness.

3.4 Optimization

Based on the developed models, an analysis on multiple response optimizations was conducted to achieve optimum results. The target is to find the optimal set of parameters within the tested range in present study that can produce a minimum surface roughness and a maximum hardness simultaneously. Different sets of optimal parameters were obtained using the desirability function approach in the Design Expert software for the optimization of multiple response processes. Different desirability functions were used based on different importance criteria of roughness and hardness. The criteria of the desirability function are intended to achieve different sets of optimal parameters that may produce roughnesses below 10 μm. A total of five experimental runs were selected and performed for optimal set of parameters as shown in Table 7. Furthermore, these different combinations of optimal parameters were used to validate the robustness of the developed empirical models. Table 7 shows the results of optimization for actual and predicted R_a as well as HV based on different importance criteria for each response. The predicted responses for both R_a and HV were calculated from the empirical models. From the Design Expert software, the minimum overall desirability function was found to be 82 %. All responses were predicted to be within these desired limits. Overall, the predicted and actual responses for both R_a and HV are satisfactory with good reliability. It shows that the models are workable in predicting the responses of R_a and HV in the present research.

4 Conclusions

Based on the Box–Behnken experimental design approach, a conclusion on the effect of multiple jet passes as well as pressure, feedrate, and standoff distance in the WJP process of aluminum alloy 5005 can be drawn as follows:

1. The roughnesses were obtained between 0.51 and 16.42 μm and the results were divided into three different groups. The first group with low roughnesses below 1 μm shows almost no erosion. The second group with a range of roughness between 1 and 10 μm shows discontinuous erosion with no constant width of erosion tracks. The third group with high roughnesses above 10 μm shows high amount of removed material with a constant width of erosion track.
2. Increasing the number of passes, pressure, and standoff distance produces a higher surface roughness as well as hardness. On the contrary, increasing the feedrate produces a lower surface roughness and hardness.
3. For specimens with low and moderate roughnesses, the magnitude of hardness is the highest at the surface and decreases with increasing depth from the surface. However, for specimens with high roughnesses, the maximum increase in hardness is not located just below the eroded surface. It was recorded at a depth of approximately 80–120 μm.
4. The developed empirical models for R_a and HV have reasonable correlations between the measured and predicted responses with acceptable R^2 and R^2_{adj}. A proper selection of peening parameters can be formulated to be used in practical works.
5. Different sets of optimal parameters were generated based on different desirability functions for each response. The predicted and actual responses for optimized R_a and HV are satisfactory with good reliability. It shows that the models are workable in predicting the responses of R_a and HV in the present research.

Acknowledgments The authors would like to gratefully acknowledge the contribution of the Institute for Manufacturing Technology

and Production Systems (Prof. Dr.-Ing. Jan C. Aurich) and the Institute for Measurement and Sensor-Technology (Prof. Dr.-Ing. Jörg Seewig), University of Kaiserslautern, for providing technical support.

References

1. Daoming G, Jie C (2006) ANFIS for high-pressure waterjet cleaning prediction. Surf Coat Technol 201:1629–1634
2. Cui L, An L, Gong W, Jiang H (2007) A novel process for preparation of ultra-clean micronized coal by high pressure water jet comminution technique. Fuel 86:750–757
3. Arola D, McCain ML, Kunaporn S, Ramulu M (2002) Waterjet and abrasive waterjet surface treatment of titanium: a comparison of surface texture and residual stress. Wear 249:943–950
4. Ramulu M, Arola D (1994) The influence of abrasive waterjet cutting conditions on the surface quality of graphite/epoxy laminates. Int J Mach Tools Manuf 34:295–313
5. Cadavid-Giraldo R (2004) Cutting with fluidjets of small diameter. Dissertation, Technische Universität Kaiserslautern
6. Meguid SA, Shagal G, Stranart JC (1999) Finite element modelling of shot-peening residual stresses. J Mater Process Technol 92–93:401–404
7. Eftekhari A, Talia JE, Mazumdar PK (1995) Influence of surface condition on the fatigue of an aluminium-lithium alloy (2090-T3). Mater Sci Eng, A 199:L3–L6
8. Braisted W, Brockman R (1999) Finite element simulation of laser shock peening. Int J Fat 21:719–724
9. Ding K, Ye L (2006) Simulation of multiple laser shock peening of a 35CD4 steel alloy. J Mater Process Technol 178:162–169
10. Grinspan AS, Gnanamoorthy R (2006) A novel surface modification technique for the introduction of compressive residual stress and preliminary studies on Al alloy AA6063. Surf Coat Technol 201:1768–1775
11. Chillman A, Ramulu M, Hashish M (2007) Waterjet peening and surface preparation at 600 MPa: a preliminary experimental study. J Fluids Eng 129:485–490
12. Ju DY, Han B (2009) Investigation of water cavitation peening-induced microstructures in the near-surface layer of pure titanium. J Mater Process Technol 209:4789–4794
13. Qin M, Ju DY, Oba R (2006) Investigation of the influence of incidence angle on the process capability of water cavitation peening. Surf Coat Technol 201:1409–1413
14. Azhari A, Schindler C, Kerscher E, Grad P (2012) Improving surface hardness of austenitic stainless steel using waterjet peening process. Int J Adv Manuf Technol. doi:10.1007/s00170-012-3962-1
15. Seeberger© (2012) Material data sheet 3.3315. Seeberger GmbH & Co. KG. http://www.seeberger.net/_assets/pdf/werkstoffe/aluminium/en/3.3315.pdf. Accessed 23 May 2012
16. Macodiyo DO, Soyama H (2006) Optimization of cavitation peening parameters for fatigue performance of carburized steel using Taguchi methods. J Mater Process Technol 178:234–240
17. Rajesh N, Ramesh BN (2005) Empirical modelling of water-jet peening of 6063-T6 aluminium alloy. J Produc Eng 86:22–26
18. Chi G, Hu S, Yang Y, Chen T (2012) Response surface methodology with prediction uncertainty: a multi-objective optimization approach. Chem Eng Res Des. doi:10.1016/j.cherd.2011.12.012
19. Alao A-R, Konneh M (2012) Surface finish prediction models for precision grinding of silicon. Int J Adv Manuf Technol 58:949–967
20. Montgomery DC, Peck EA, Vining GG (2001) Introduction to linear regression analysis. Wiley, New York
21. Wang J, Guo DM (2003) The cutting performance in multipass abrasive waterjet machining of industrial ceramics. J Mater Process Technol 133:371–377
22. Oka YI, Mihara S, Miyata H (2007) Effective parameters for erosion caused by water droplet impingement and applications to surface treatment technology. Wear 263:386–394
23. Chillman A, Ramulu M, Hashish M (2010) Waterjet and water-air jet surface processing of a titanium alloy: a parametric evaluation. J Manufac Scie Eng 132:011012
24. Azmir MA, Ahsan AK (2009) A study of abrasive water jet machining process on glass/epoxy composite laminate. J Mater Process Technol 209:6168–6173
25. Fowlkes WY, Creveling CM (1995) Engineering methods for robust product design: using Taguchi methods in technology and product development. Addison-Wesley, Massachusetts
26. Grinspan AS, Gnanamoorthy R (2006) Surface modification by oil jet peening in Al alloys, AA6063-T6 and AA6061-T4: residual stress and hardness. App Surf Sci 253:989–996